Three-dimensional Ising behavior of antiferromagnetic Bi_2CuO_4

B. D. White, W. M. Pätzold,* and J. J. Neumeier
Department of Physics, Montana State University, P.O. Box 173840, Bozeman, Montana 59717-3840, USA
(Received 26 July 2010; revised manuscript received 26 August 2010; published 23 September 2010)

Bi_2CuO_4 possesses a unique crystal structure that distinguishes it from other cuprates. It is constructed from isolated CuO_4 plaquettes forming staggered chains along the c axis of its tetragonal unit cell. Several aspects of antiferromagnetism in this system, observed below $T_N \sim 43$ K, are poorly understood, including the orientation of the ordered magnetic moments. There is disagreement about whether Bi_2CuO_4 exhibits easy-axis or easy-plane anisotropy despite numerous attempts to settle the question. In order to better understand its magnetism, thermal expansion and heat capacity were measured on a single crystal of Bi_2CuO_4, and the critical behavior exhibited about T_N in those measurements was carefully studied. Best-fit values for the critical exponent α and the ratio of the leading singularity amplitudes A_+/A_- from thermal-expansion data along both a and c are consistent with the three-dimensional Ising universality class. Assignment of the Ising universality class suggests Bi_2CuO_4 is an easy-axis antiferromagnet with moments ordered along c.

DOI: 10.1103/PhysRevB.82.094439 PACS number(s): 75.40.−s, 65.40.De, 74.72.−h

I. INTRODUCTION

Despite an absence of superconductivity, Bi_2CuO_4 received considerable attention during the cuprate physics boom following the discovery of high-temperature superconductivity. Interest was driven by its unique crystal structure and the consequences thereof. One might expect Bi_2CuO_4 to be isostructural with La_2CuO_4, especially given nearly identical ionic radii for Bi^{3+} and La^{3+} with eightfold coordination.[1,2] However, strongly covalent Bi-O bonds reduce the coordination of Bi to six while the strongly ionic nature of La-O bonds allow for ninefold coordination.[1] Definitive early x-ray diffraction work[3] revealed a tetragonal unit cell with space group $P4/ncc$. This result has been unambiguously confirmed by neutron-diffraction[1,4–7] and Raman infrared-reflectivity[8] experiments. The crystal structure, which is displayed in Figs. 1(a) and 1(b) as generated by JAVA STRUCTURE VIEWER,[9] is unique among the generally two-dimensional, layered cuprates. It is constructed from isolated CuO_4 plaquettes which form staggered, colinear "chains" along c, connected by BiO_4 units,[10,11] with a twist angle[7] of 33.3° between adjacent plaquettes. The isolated nature of CuO_4 plaquettes has led some to refer to Bi_2CuO_4 as a "zero-dimensional" compound. For example, a study of the intensity of Cu $2p_{5/2}$ core-level x-ray photoemission spectra demonstrated that CuO_4 plaquettes result in a low-dimensional behavior that is fundamentally different from those arising from CuO_3 chains (one-dimensional) and CuO_2 planes (two-dimensional).[12]

Like other cuprates, the $S=\frac{1}{2}$, Cu^{2+} moments of Bi_2CuO_4 undergo antiferromagnetic order as observed around 43 K in neutron-diffraction,[1,5–7] antiferromagnetic-resonance,[1] and magnetic-susceptibility experiments.[1,6,13] Four distinct Cu-O-Bi-O-Cu superexchange paths have been identified, which are responsible for magnetic order,[1,7,11,14,15] however, there remain disagreements about the orientation of the ordered moments.[10] Tetragonal antiferromagnets with anisotropic exchange are said to exhibit easy-axis anisotropy when their sublattices are polarized parallel to c and easy-plane anisotropy when they are polarized perpendicular to c. In the case of Bi_2CuO_4, it is known that magnetic moments order ferromagnetically within the chains running along c and that neighboring chains are antiferromagnetically coupled. However, despite numerous attempts to settle the matter, there is still disagreement about whether the magnetic moments order parallel (easy-axis anisotropy)[7,10,14,16] or perpendicular (easy-plane anisotropy)[4,11,17,18] to the chains. One way to resolve this issue that has been ignored until now is to identify the universality class to which the antiferromagnetic phase

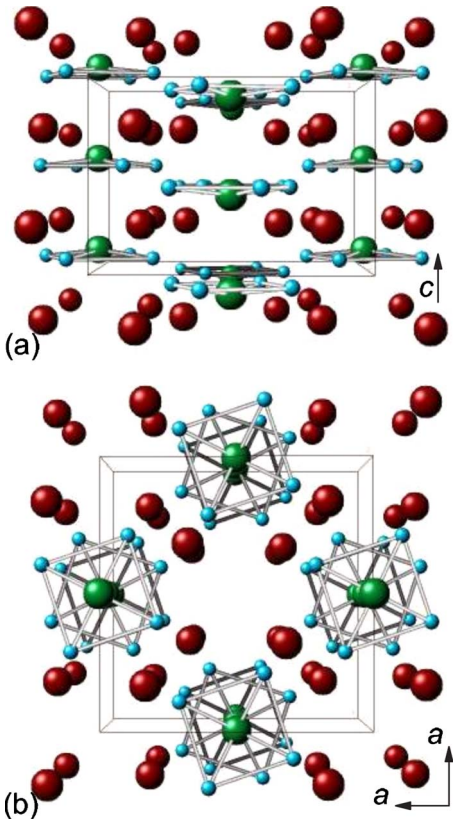

FIG. 1. (Color online) (a) Isolated CuO_4 plaquettes form colinear chains along c, which are connected by BiO_4 units and (b) looking down along the chains.

transition in Bi_2CuO_4 belongs. To this end, we have measured the thermal expansion and heat capacity of single-crystal Bi_2CuO_4 in order to study its critical behavior. We have extracted the critical exponent α and ratio of the leading singularity amplitudes A_+/A_- from these measurements and found that they correlate well with predictions for the three-dimensional Ising model. This universality class assignment is consistent with easy-axis anisotropy.

II. EXPERIMENT

Single-crystalline Bi_2CuO_4 was grown by the floating-zone method. Polycrystalline rods containing 1% CuO excess were synthesized from oxide starting materials Bi_2O_3 (99.99%) and CuO (99.995%). The powder was reacted in air at 600, 650, 700, and 725 °C for 24 h each, between which it was subjected to grinding by mortar and pestle and planetary ball milling for 2 h at 200 rpm. Polycrystalline rods were pressed by hand using a previously described technique,[19] except that quartz tubes were substituted for alumina tubes due to their less reactive interface with the pressed rod. The pressed rods were reacted a final time at 750 °C for 24 h.

Growth parameters were selected to replicate conditions for the floating-zone growth of Bi_2CuO_4 as published in Ref. 20. Crystal growth was conducted in air (1 atm) with a 10 mm/h growth rate and 30 rpm counterrotation. The surface tension of molten Bi_2CuO_4 is too low to maintain a stable molten zone throughout the course of a long, slow growth which explains previous use[20] of a rather fast growth rate. We found that a 5 mm/h growth speed yielded higher-quality crystalline boules than those grown at 10 mm/h, though growing at lower speeds required constant adjustments to the molten zone. All grown boules had an affinity for cleaving to reveal the (00*l*) plane and seemed to grow approximately along [1 0 2]. Samples were cut from the boule, oriented by back-reflection Laue diffraction, and polished to form a parallelepiped with faces perpendicular to the principal crystallographic directions.

High-resolution thermal expansion and heat capacity were measured on samples originating from the same crystal. Thermal expansion was measured using a dilatometer cell, constructed from fused quartz, which is sensitive to total length changes on the order of 0.1 Å.[21] The sample used in our dilatometry measurements was 3.191 mm along *a* and 1.696 mm along *c*. Data were collected on warming while sweeping the temperature at a rate of 0.20(1) K/min. Heat capacity was measured using the physical properties measurement system heat-capacity option from Quantum Design which uses a thermal relaxation technique.

III. RESULTS AND DISCUSSION

Linear thermal expansion $\Delta L/L$ along *a* and *c* was measured on warming and the resulting data are displayed in Fig. 2. The raw data were corrected only for the thermal expansion of quartz, from which the dilatometer cell is constructed, and for the empty cell effect as described in Ref. 21. The coefficient of thermal expansion, $\mu = d(\Delta L/L)/dT$, is obtained from point-by-point differentiation of $\Delta L/L$ without prior processing or smoothing of the data and is displayed in Fig. 3. Ignoring, for now, the effect of antiferromagnetic order on $\Delta L/L$ and μ around 43 K, we observe significant anisotropy. Tetragonal Bi_2CuO_4 belongs to the class of axial crystal structures which always exhibit two unique thermal-expansion coefficients $\mu_\parallel$ and $\mu_\perp$ taken to be along *c* and *a*, respectively. The ratio of $\mu_\parallel$ and $\mu_\perp$ is an excellent measure of anisotropy and is expressed as[22,23]

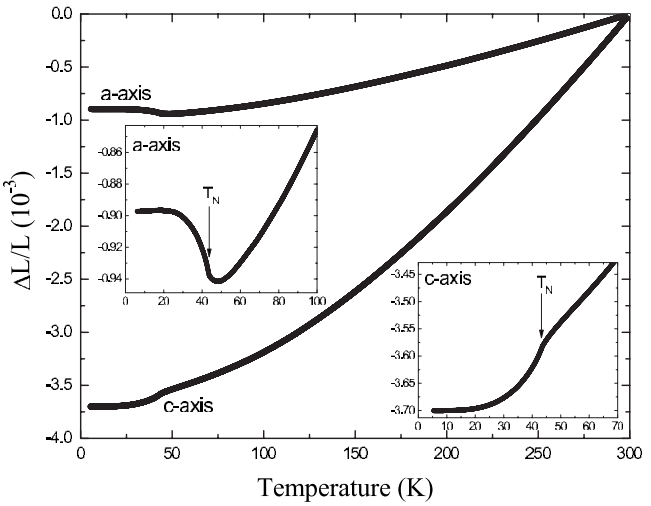

FIG. 2. Linear thermal expansion $\Delta L/L$ along *a* and *c* between 5 and 300 K. The insets display the behavior along both axes in the vicinity of the antiferromagnetic phase transition (T_N denoted by arrow).

$$\frac{\mu_\parallel}{\mu_\perp} = \frac{(C_{11}+C_{12})\gamma_\parallel - 2C_{13}\gamma_\perp}{C_{33}\gamma_\perp - C_{13}\gamma_\parallel}. \quad (1)$$

$\mu_\parallel/\mu_\perp$ is a function of elastic constants and the weighted mean Grüneisen parameters $\gamma_\parallel$ and $\gamma_\perp$, which are averaged over individual Grüneisen parameters $\gamma_{\parallel,j}$ and $\gamma_{\perp,j}$ (for the

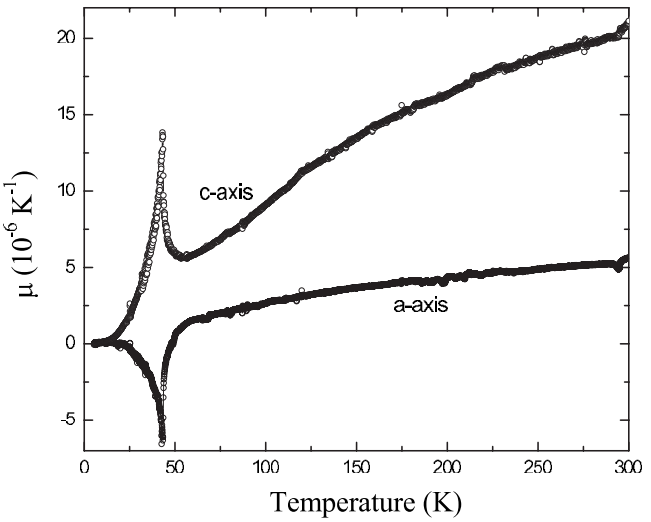

FIG. 3. Linear coefficient of thermal expansion, defined by $\mu = d(\Delta L/L)/dT$, along *a* and *c*.

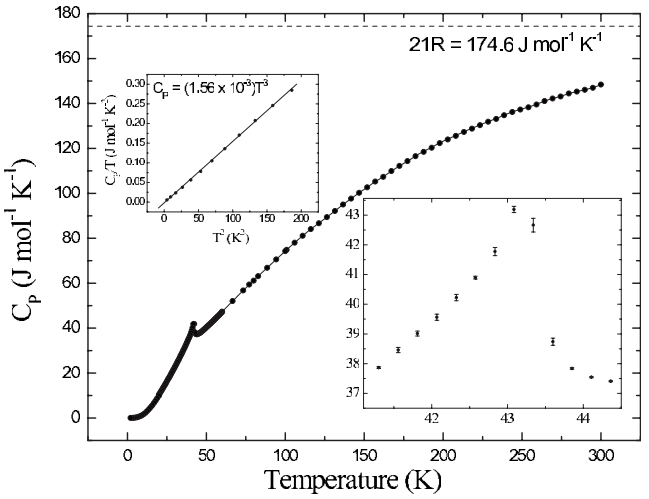

FIG. 4. Heat capacity of Bi_2CuO_4. Note that the line in the main figure is not a fit but is rather a guide to the eyes. The upper inset highlights the T^3 dependence of C_P at low temperature by fitting a line through a plot of C_P/T against T^2. The lower inset highlights the anomaly around T_N.

jth phonon mode) and weighted by the heat-capacity contribution C_j of that mode.[24] A crystal described by space group $P4/ncc$ (D^8_{4h}) has six independent elastic constants.[25] Equation (1) contains four of them omitting only C_{44} and C_{66} because they result in rotation of the crystal. Examination of Eq. (1) suggests that the observed anisotropic thermal expansion arises from the interplay of thermal stress coefficients (proportional to γ) and elastic constants.[22] Unfortunately, we cannot compare the results of Eq. (1) with our data because the elastic constants of Bi_2CuO_4 have not been measured. Instead, we compare the observed anisotropy to other sources. For example, neutron-diffraction experiments show a reduction in the lattice parameters between 290 and 1.5 K of 0.0588(2)% and 0.393(2)% along a and c, respectively.[7] These are consistent with our measurements[26] of $\Delta L/L$ which show reductions of 0.07(2)% and 0.371(1)% between 300 and 5 K along those same directions. Furthermore, refinements of thermal parameters from neutron diffraction exhibit an anisotropy wherein the thermal motion of Bi, Cu, and O ions is $\sim 3-4$ times larger along c than along a.[5,7] This implies that the lattice is stiffer along a than along c which is also in agreement with our measurements.

The heat capacity of Bi_2CuO_4 is displayed in Fig. 4. Our results are consistent with previous publication of C_P data for this system.[27] At low temperature, the data were successfully described by $C_P=\beta T^3$ (see upper inset of Fig. 4), where $\beta=\beta_{\rm Ph}+\beta_{\rm AFM}$ represents, in general, a combination of phonon and antiferromagnetic spin-wave contributions to C_P.[28] Attempts to extract a linear temperature term representing electronic degrees of freedom were predictably unsuccessful given the compound's insulating ground state (2 eV band gap).[29] Neutron-diffraction studies of spin-wave dispersion in Bi_2CuO_4 demonstrate the existence of a 2.1 meV $\simeq$24.4 K energy gap of the lowest-energy spin-wave branch at the zone center.[4] Therefore, our low-temperature fit of C_P (2–13.5 K) is expected to be free of any spin-wave contribution and is dominated by phonons ($\beta=\beta_{\rm Ph}$). The Debye temperature of Bi_2CuO_4 is a function of $\beta_{\rm Ph}$ and is calculated $\Theta_D \simeq 108$ K from our optimized $\beta=1.56\times10^{-3}$ J mol^{-1} K^{-4}. At high temperature ($T \gg \Theta_D$), C_P asymptotes toward $21R \simeq 174.6$ J mol^{-1} K^{-1} which is signified by a dashed line in Fig. 4. This asymptotic value is predicted by the classic Dulong-Petit law for a compound with seven ions per formula unit.

In the vicinity of T_N, anomalies corresponding to antiferromagnetic ordering of Cu^{2+} spins are observed in $\Delta L/L$ and μ along each principal crystallographic axis (Figs. 2 and 3) and in C_P (Fig. 4). In the case of $\Delta L/L$, the anomalies are characterized by an abrupt change in slope and are highlighted in the upper and lower insets of Fig. 2. The minimum along a indicates the onset of negative thermal expansion and should not be confused with T_N. Lambda-like anomalies are observed in μ and C_P in Figs. 3 and 4, respectively. The anomalies in μ exhibit a commonly observed anisotropy wherein the peaks have opposite sign.[30,31]

C_P and the volume coefficient of thermal expansion Ω ($\Omega=2\mu_a+\mu_c$) scale in the vicinity of T_N in the case of a continuous phase transition. The scaling relation,[32]

$$C_P^* \simeq \lambda \Omega T, \tag{2}$$

is commonly referred to as a Pippard relation, where $C_P^* \equiv C_P - f(T)$ and $f(T)=a-bT$ is a linear background.[33] λ is a scaling constant with units of joule per mole per kelvin which is inversely proportional to the pressure derivative of the transition temperature $dT_N/dP=\nu/\lambda$, where ν is molar volume.[32] For Bi_2CuO_4, satisfactory scaling between ΩT and C_P^* (not shown) is achieved for $\lambda=-3.96(4)\times10^4$ J mol^{-1} K^{-1}. We calculate $dT_N/dP=-1.59(2)$ K GPa^{-1} where we have used $\nu=6.30\times10^{-5}$ m^3 mol^{-1}. Unfortunately, there are no direct measurements of dT_N/dP for Bi_2CuO_4 with which we can compare this calculation but our value is the same order of magnitude as other antiferromagnets.[30,31]

Satisfaction of the scaling relation $C_P^* \simeq \lambda\Omega T$ implies that any expression used to study the critical behavior of C_P may be used with equal justification to study $\lambda\Omega T$.[30–32,34,35] The canonical expression for critical behavior we shall employ is

$$\lambda\Omega T \simeq \frac{A_\pm}{\alpha}|t|^{-\alpha}(1+E_\pm|t|^\chi)+B+Dt, \tag{3}$$

where $\chi=0.5$, $t\equiv(T-T_N)/T_N$ is the reduced temperature, and plus-minus subscripts represent quantities which are different above (+) and below (−)T_N, respectively. However, instead of studying the volume behavior of ΩT with Eq. (3), we chose to study the behavior along the two distinct crystallographic axes ($\mu_a T$ and $\mu_c T$). It has been established for a few cases[35] that the characteristic elements of critical behavior, including α and A_+/A_-, are identical along distinct crystallographic axes. This result makes a general intuitive sense but it would be interesting to determine whether or not it holds for Bi_2CuO_4. If it does hold true, we have two *independent* data sets from which we can extract information about its critical behavior.

TABLE I. Least-squares best-fit values for parameters in Eq. (3) along a and c for various constraints.

Axis	Constraint	A_- [a]	A_+/A_-	α	E_-	E_+	B [a]	D [a]
a	$E_-=E_+=0$	4.31(5)	0.737(6)	0.130(1)	0.0	0.0	−30.003	1.4(8)
a	$E_-=E_+\neq 0$	3.8(2)	0.73(4)	0.096(3)	−0.34(2)	−0.34(2)	−29(1)	−0.5(5)
a	$E_-\neq E_+\neq 0$	2.69(3)	0.693(4)	0.111(1)	−0.53(1)	−1.69(2)	−9.5168	24.3(5)
c	$E_-=E_+=0$	0.65(2)	0.77(1)	0.109(2)	0.0	0.0	−3.6610	8.6(2)
c	$E_-=E_+\neq 0$	0.39(6)	0.6(1)	0.11(1)	−1.2(1)	−1.2(1)	0.7(4)	5.9(3)
c	$E_-\neq E_+\neq 0$	0.556(6)	0.64(1)	0.111(5)	−0.75(1)	0.13(2)	−1.53(9)	2.7(1)

[a]Units of joule per mole per kelvin.

We employ a Levenberg-Marquardt algorithm (nonlinear least squares) to fit each μT data set around T_N with the critical expression in Eq. (3). The data we studied ($\lambda_a\mu_a T$ and $\lambda_c\mu_c T$) were multiplied by scaling constants $\lambda_a=-1.0\times 10^5$ and $\lambda_c=1.0\times 10^4$ instead of $\lambda=-39\,600$. These values were chosen purely for convenience and have no physical significance. We see from Eq. (3) that we can multiply through by a constant without influencing fit parameters except for $A_\pm$, B, and D (no influence on α and A_+/A_-, for example). When we wish to compare best-fit parameters from the fits along each axis which are sensitive to the scaling constant, we first multiply each by an appropriate constant so that $\lambda_a=\lambda_c$.

The experimental uncertainty of our μT data was estimated from the standard deviation of the residuals (which exhibit reasonably Gaussian characteristics) of a sixth-order Chebyshev polynomial fit to the data in the critical temperature regime. This uncertainty was inserted into the chi-square minimization function, from where it propagates into the best-fit parameter uncertainties. We have adhered to the customary practice[36] of identifying the square root of the diagonal elements of the formal covariance matrix with the statistical standard errors of the best-fit parameters. This is justifiable so long as our measurement errors are truly Gaussian, which we believe to be the case.

We performed an identical procedure for fitting the critical expression [Eq. (3)] to our μT data along each axis. This procedure began by ignoring corrections to scaling and considering instead a simple case where we constrain $E_-=E_+=0$. This constraint limits the temperature range over which the data may be fit, but allows us to get an initial estimate of the critical temperature regime by adjusting the fitted temperature range until it was maximized while still producing an acceptable fit to the data. We then allowed E_- and E_+ to be different from zero, which increases the fittable temperature range. In order to account for all possibilities, we considered two cases: application of the constraint $E_-=E_+$ and relaxing that constraint so that $E_-\neq E_+$.

The resulting fits for the three cases along both axes are displayed in Table I. The first thing we observe is that α and A_+/A_- are similar in all six fits which implies that the critical behavior along the two independent, principal crystallographic directions does appear to be the same. Some of the parameters have no uncertainty listed. We observed strong correlations between $A_\pm$ and B which resulted in large covariances between them and absurdly large calculated uncertainties. In those cases, we chose to fix B at its best-fit value and refit the data over the remaining parameters. This procedure results in much lower uncertainties which certainly underestimate the true uncertainty but nonetheless are more reasonable. Negative values for the analytic background terms (B and D) in many of the fits may appear unphysical. Certainly, when fitting the critical behavior of C_P, the analytic background parameters *must* be positive. However, if we examine the scaling relation $C_P=\lambda\Omega T+f(T)$, we see that we should consider the analytic background of $\lambda\Omega T=2(\lambda/\lambda_a)\mu_a T+(\lambda/\lambda_c)\mu_c T$ and then add $f(T)$ to it to yield the effective background associated with C_P. When we perform this calculation with our best-fit values, the resulting linear background is perfectly consistent with expectations that its slope and intercept be positive. There is no such expectation, however, for the individual backgrounds of each μT data set.

Noticeably absent from Table I are values for T_N. We found that allowing T_N to vary as a fittable parameter, led to our algorithm's failure to converge to a least-squares solution. So instead, we fixed T_N at reasonable values and found a narrow temperature range over which fits were optimized. We repeated this procedure for each fit in Table I finding that the optimized T_N values were 43.381(1) K. Therefore, we chose to simply fix $T_N=43.381$ K for each fit.

We display the critical behavior fits (case where $E_-\neq E_+\neq 0$) and our $\lambda_a\mu_a T$ and $\lambda_c\mu_c T$ data in Fig. 5. Small oscillations in the measured data around 45–50 K are a consequence of our dilatometer's remarkable sensitivity to modest 10 mK/min oscillations about our 0.2 K/min warming rate in that temperature region. The fits in each case are good over a reduced temperature range of $\sim\log|t|=-0.75$ to $\sim\log|t|=-2.0$. A high-quality single crystal with a magnetic transition should exhibit a critical temperature range that begins by $\sim\log|t|=-1.0$ and ends close to $\log|t|=-4.0$ where even modest crystalline defects begin to influence critical behavior.[37] It may then be tempting to discount our results which penetrate the critical region no further than about $\log|t|=-2.0$ by claiming the sample quality and/or measurements were poor. However, neither of these explanations is accurate. Our limited critical region is largely a consequence of numerically differentiating $\Delta L/L$ to yield μ.[38] Simple numerical differentiation of $f(T)$ proceeds by using the first term of the infinite series expansion (in powers of ΔT)

$$f'(T)\simeq\frac{f(T+\Delta T)-f(T)}{\Delta T}+\mathcal{O}(\Delta T), \tag{4}$$

where ΔT is the data density (temperature difference between neighboring data) and $\mathcal{O}(\Delta T)$ represents the series ex-

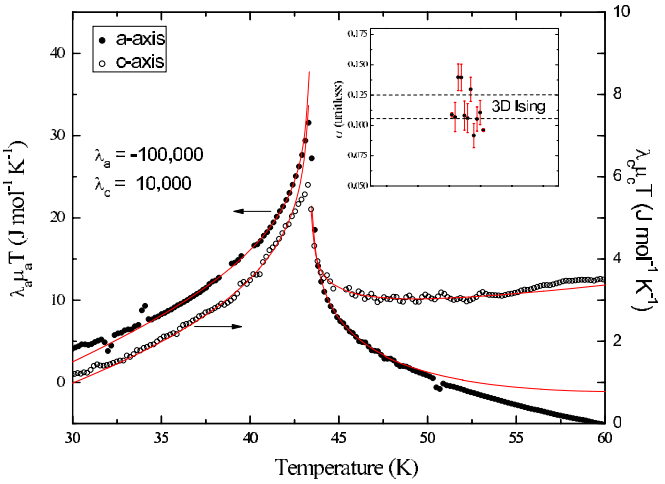

FIG. 5. (Color online) $\lambda_a\mu_a T$ and $\lambda_c\mu_c T$ (closed and open circles, respectively) in the vicinity of T_N and their respective fits (red line) to Eq. (3). The inset displays α from fits over maximized temperature ranges (results in Table I) as well as some smaller temperature ranges, assuming a variety of constraints on $E_\pm$ for both a- and c-axis data. The horizontal lines indicate a range of expected values for the three-dimensional Ising universality class as calculated by various approximation methods.

pansion with its leading term of order ΔT. In the limit $\Delta T \rightarrow 0$, the higher-order terms vanish and we yield the traditional definition of a point-by-point derivative. However, if ΔT is finite, as it is in all measurements, truncating the series results in an error[36] η which is dominated by the leading truncated term $\eta = -\frac{1}{2}f''(T)\Delta T$. The presence of a nonzero η tends to broaden the transition in the region immediately around T_N and to cut down the singularity's height.[38] These two effects conspire to obscure the true critical behavior as T_N is approached, causing premature deviation from the expected behavior. We address these issues in detail in a manuscript which is currently in preparation.[38] Despite a somewhat limited critical region, there is no doubt that our fits are probing the true critical behavior of the system, and though we would prefer to have a more expanded temperature range, our analysis and results remain valid.

The values of α and A_+/A_- from our fits as summarized in Table I are not only self-consistent with one another, they are consistent with expected behavior for the three-dimensional Ising universality class. Unfortunately, there is not an exact solution for the Ising model in three spatial dimensions, however, a variety of techniques have been employed to yield approximate values for α and A_+/A_-. Pelissetto and Vicari[39] summarize the results of numerous three-dimensional Ising model studies including 21 which employ the high-temperature series-expansion technique, 24 using Monte Carlo simulations, and 11 using low-temperature series expansions. If we average the results for each technique, we find $\alpha = 0.108(2)$, $\alpha = 0.112(4)$, and $\alpha = 0.121(4)$, respectively, which provides a range $0.106 \leq \alpha \leq 0.125$. The inset of Fig. 5 displays the results for α from Table I (fit over maximized temperature ranges) along with other values obtained from fits over smaller temperature ranges and with various constraints on $E_\pm$. These values mostly fall within the range between 0.106 and 0.125. Furthermore, our values for A_+/A_- from Table I are also most consistent with the three-dimensional Ising universality class. Expansions to second order in ϵ where $\epsilon = 4-d$ and d is the lattice dimensionality, lead to A_+/A_- values[40] of 0.52(1), 1.03(1), and 1.52(2) for an order parameter with one, two, and three dimensions, respectively, assuming a three-dimensional lattice ($\epsilon = 1$). Our least-squares fits give $A_+/A_- \sim 0.7$ which is closest to a one-dimensional order parameter (Ising model). Therefore, we can say that both α and A_+/A_- correlate most closely with the three-dimensional Ising model.

Identification of Bi_2CuO_4 as a three-dimensional Ising antiferromagnet distinguishes it from other 214 cuprates which are generally classified among two-dimensional Heisenberg systems. More importantly, it suggests that Bi_2CuO_4 is an easy-axis antiferromagnet with its magnetic moments polarized parallel to c. This conclusion is consistent with theory[10,16] and two-magnon Raman[14] studies while torque magnetometry[17] and antiferromagnetic resonance[13,18] experiments offer the strongest and most compelling support for the opposite conclusion of easy-plane anisotropy. Compared with these latter experiments, we feel our study of critical behavior is, perhaps, a more straightforward method to address the easy-axis vs easy-plane anisotropy problem in Bi_2CuO_4 because we arrived at our conclusion without invoking any prior assumptions about the details of its magnetic order. In any case, our result should help to settle the issue of magnetic anisotropy in Bi_2CuO_4 as future studies investigate this question further.

IV. CONCLUSION

We have measured thermal expansion and heat capacity on single-crystal samples of Bi_2CuO_4 in order to study the critical behavior of its antiferromagnetic transition. By employing a scaling relation between C_P and ΩT, we were able to fit the critical behavior exhibited by our measurements of thermal expansion with an expression derived for heat capacity. The results of the scaling analysis allowed us to calculate the pressure derivative of the Néel temperature $dT_N/dP = -1.59(2)$ K GPa^{-1}. As a consequence of our choice to study the thermal expansion coefficients along a and c rather than the volumetric coefficient of thermal expansion, we were able to show that the critical behavior along both axes was identical and, therefore, we had two *independent* data sets from which we could extract α and A_+/A_-. We performed nonlinear least-squares fitting under a variety of constraints and all our results are consistent with the three-dimensional Ising universality class. This classification suggests Bi_2CuO_4 exhibits easy-axis anisotropy.

ACKNOWLEDGMENTS

This material is based upon work supported by the U.S. Department of Energy Office of Basic Energy Sciences (Grant No. DE-FG-06ER46269) and the National Science Foundation (Grant No. DMR-0907036). Helpful discussions with R. K. Bollinger are gratefully acknowledged. We also thank H. V. Schmidt for use of his planetary ball mill.

*Permanent address: Georg-August-Universität Göttingen, Fakultät für Physik, Friedrich-Hund-Platz 1, 37077 Göttingen, Germany.

[1] E. W. Ong, G. H. Kwei, R. A. Robinson, B. L. Ramakrishna, and R. B. von Dreele, Phys. Rev. B **42**, 4255 (1990).

[2] R. D. Shannon and C. T. Prewitt, Acta Crystallogr., Sect. B: Struct. Crystallogr. Cryst. Chem. **25**, 925 (1969).

[3] J. C. Boivin, J. Tréhoux, and D. Thomas, Bull. Soc. Fr. Mineral. Cristallogr. **99**, 193 (1976).

[4] B. Roessli, P. Fischer, A. Furrer, G. Petrakovskii, K. Sablina, V. Valkov, and B. Fedoseev, J. Appl. Phys. **73**, 6448 (1993).

[5] J. Konstantinovic, G. Stanisic, M. Ain, and G. Parette, J. Phys.: Condens. Matter **3**, 381 (1991).

[6] R. Troć, J. Janicki, I. Fiłatow, P. Fischer, and A. Murasik, J. Phys.: Condens. Matter **2**, 6989 (1990).

[7] J. L. García-Muñoz, J. Rodríguez-Carvajal, F. Sapiña, M. J. Sanchis, R. Ibáñez, and D. Beltrán-Porter, J. Phys.: Condens. Matter **2**, 2205 (1990).

[8] Z. V. Popović, G. Kliche, M. Cardona, and R. Liu, Phys. Rev. B **41**, 3824 (1990).

[9] S. Weber, J. Appl. Crystallogr. **32**, 1027 (1999).

[10] O. Janson, R. O. Kuzian, S.-L. Drechsler, and H. Rosner, Phys. Rev. B **76**, 115119 (2007).

[11] M. Aïn, G. Dhalenne, O. Guiselin, B. Hennion, and A. Revcolevschi, Phys. Rev. B **47**, 8167 (1993).

[12] C. Waidacher, J. Richter, and K. W. Becker, Phys. Rev. B **61**, 13473 (2000).

[13] G. A. Petrakovskii, K. A. Sablina, A. I. Pankrats, V. M. Vorontinov, A. Furrer, B. Roessli, and P. Fischer, J. Magn. Magn. Mater. **140-144**, 1991 (1995).

[14] M. J. Konstantinović, Z. Konstantinović, and Z. V. Popović, Phys. Rev. B **54**, 68 (1996).

[15] D. F. Khozeev, A. A. Gippius, E. N. Morozova, A. N. Vasil'ev, A. V. Zalessky, W. Hoffmann, K. Lüders, G. Dhalenne, and A. Revcolevschi, Physica B **284-288**, 1377 (2000).

[16] N. Tanaka, Y. Hirota, T. Kawakami, and K. Motizuki, J. Magn. Magn. Mater. **177-181**, 1387 (1998).

[17] M. Herak, M. Miljak, G. Dhalenne, and A. Revcolevschi, J. Phys.: Condens. Matter **22**, 026006 (2010).

[18] A. I. Pankrats, D. Y. Sobyanin, A. M. Vorotinov, and G. A. Petrakovskii, Solid State Commun. **109**, 263 (1999).

[19] B. D. White, C. A. M. dos Santos, J. A. Souza, K. J. McClellan, and J. J. Neumeier, J. Cryst. Growth **310**, 3325 (2008).

[20] G. Dhalenne, A. Revcolevshi, M. Ain, B. Hennion, G. Andre, and G. Parette, Cryst. Prop. Prep. **36-38**, 11 (1991).

[21] J. J. Neumeier, R. K. Bollinger, G. E. Timmins, C. R. Lane, R. D. Krogstad, and J. Macaluso, Rev. Sci. Instrum. **79**, 033903 (2008).

[22] G. D. Barrera, J. A. O. Bruno, T. H. K. Barron, and N. L. Allan, J. Phys.: Condens. Matter **17**, R217 (2005).

[23] N. A. Abdullaev, Phys. Solid State **43**, 727 (2001).

[24] Note that the Grüneisen functions associated with phonon mode j are written $\gamma_{\|,j}=-(\partial \ln \omega_j/\partial c)_a$ for out-of-plane and $\gamma_{\perp,j}=-(1/2)(\partial \ln \omega_j/\partial \ln a)_c$ for in-plane.

[25] M. Yaoming and T. Ruibao, Chin. Phys. Lett. **8**, 195 (1991).

[26] We have averaged $100\times[\Delta L/L(300\ \mathrm{K})-\Delta L/L(5\ \mathrm{K})]$ from three measurements along a and two along c to yield the percent lattice reductions along a and c between 300 and 5 K.

[27] M. Castro, R. Burriel, R. Ibañez, and F. Sapiña, IEEE Trans. Magn. **30**, 1163 (1994); A. Strejc, D. Sedmidubský, K. Růžička, and J. Leitner, Thermochim. Acta **402**, 69 (2003).

[28] A. L. Cornelius, B. E. Light, and J. J. Neumeier, Phys. Rev. B **68**, 014403 (2003).

[29] A. Goldoni, U. del Pennino, F. Parmigiani, L. Sangaletti, and A. Revcolevschi, Phys. Rev. B **50**, 10435 (1994).

[30] B. D. White, J. A. Souza, C. Chiorescu, J. J. Neumeier, and J. L. Cohn, Phys. Rev. B **79**, 104427 (2009).

[31] C. A. M. dos Santos, J. J. Neumeier, Y.-K. Yu, R. K. Bollinger, R. Jin, D. Mandrus, and B. C. Sales, Phys. Rev. B **74**, 132402 (2006).

[32] J. A. Souza, Y.-K. Yu, J. J. Neumeier, H. Terashita, and R. F. Jardim, Phys. Rev. Lett. **94**, 207209 (2005).

[33] Some contributions to C_P have a negligible impact on thermal expansion such as certain phonon modes which may still be quasiharmonic in the vicinity of T_N. These contributions can be modeled by $a+b'T$ sufficiently near to T_N. The derivation of the Pippard relation (see Ref. 32) also yields an additive term $T(\partial S/\partial T)_C$, where the derivative is the slope of the projection of the parametric entropy curve $S(T_N,P(T_N))$ on the (T,S) plane. Thus, the background we subtract is a combination of these two factors $f(T)=a+[b'+(\partial S/\partial T)_C]T$ where the term in brackets is redefined as b.

[34] J. A. Souza, J. J. Neumeier, B. D. White, and Y.-K. Yu, Phys. Rev. B **81**, 172410 (2010).

[35] J. W. Philp, R. Gonano, and E. D. Adams, Phys. Rev. **188**, 973 (1969).

[36] W. H. Press, S. A. Teukolsky, W. T. Vetterling, and B. P. Flannery, *Numerical Recipes in C* (Cambridge University Press, Cambridge, 1992).

[37] G. Ahlers, Rev. Mod. Phys. **52**, 489 (1980).

[38] B. D. White and J. J. Neumeier (unpublished).

[39] A. Pelissetto and E. Vicari, Phys. Rep. **368**, 549 (2002).

[40] C. Bervillier, Phys. Rev. B **34**, 8141 (1986).